

# Fine structure in the $\alpha$ decay of high-spin isomers in $^{155}\text{Lu}$ and $^{156}\text{Hf}$

E. Parr,<sup>1,\*</sup> R. D. Page,<sup>1</sup> D. T. Joss,<sup>1</sup> F. A. Ali<sup>†‡</sup>,<sup>1</sup> K. Auranen<sup>§</sup>,<sup>2</sup> L. Capponi<sup>¶</sup>,<sup>3,4</sup> T. Grahn,<sup>2</sup> P. T. Greenlees,<sup>2</sup> J. Henderson,<sup>5</sup> A. Herzán<sup>\*\*</sup>,<sup>2</sup> U. Jakobsson<sup>††</sup>,<sup>2</sup> R. Julin,<sup>2</sup> S. Juutinen,<sup>2</sup> J. Konki<sup>‡‡</sup>,<sup>2</sup> M. Labiche,<sup>6</sup> M. Leino,<sup>2</sup> P. J. R. Mason,<sup>6</sup> C. McPeake,<sup>1</sup> D. O'Donnell<sup>§§</sup>,<sup>1</sup> J. Pakarinen,<sup>2</sup> P. Papadakis<sup>¶¶</sup>,<sup>2</sup> J. Partanen,<sup>2</sup> P. Peura,<sup>2</sup> P. Rahkila,<sup>2</sup> J. P. Reville,<sup>1</sup> P. Ruotsalainen,<sup>2</sup> M. Sandzelius,<sup>2</sup> J. Sarén,<sup>2</sup> C. Scholey,<sup>2</sup> J. Simpson,<sup>6</sup> J. F. Smith,<sup>3,4</sup> M. Smolen,<sup>3,4</sup> J. Sorri,<sup>2</sup> S. Stolze<sup>\*\*\*</sup>,<sup>2</sup> A. Thornthwaite,<sup>1</sup> and J. Uusitalo<sup>2</sup>

<sup>1</sup>*Oliver Lodge Laboratory, University of Liverpool, Liverpool, L69 7ZE, United Kingdom*

<sup>2</sup>*University of Jyväskylä, Department of Physics,  
P.O. Box 35, FI-40014 University of Jyväskylä, Finland*

<sup>3</sup>*School of Engineering and Computing, University of the West of Scotland, Paisley, PA1 2BE, United Kingdom*

<sup>4</sup>*Scottish Universities Physics Alliance*

<sup>5</sup>*Department of Physics, University of York, Heslington, York, YO10 5DD, United Kingdom*

<sup>6</sup>*Nuclear Physics Group, STFC Daresbury Laboratory,  
Daresbury, Warrington WA4 4AD, United Kingdom*

(Dated: August 23, 2018)

Fine structure in the  $\alpha$  decay of high-spin isomers in  $^{155}\text{Lu}(25/2^-)$  and  $^{156}\text{Hf}(8^+)$  has been studied for the first time using  $\alpha\gamma$ -coincidence analysis. Three new  $\alpha$  decays from  $^{155}\text{Lu}(25/2^-)$  and two from  $^{156}\text{Hf}(8^+)$  have been identified, populating seniority  $s > 1$  states in the  $N = 82$  nuclei  $^{151}\text{Tm}$  and  $^{152}\text{Yb}$ , respectively. The reduced hindrance factors of the  $\alpha$  decays support the previous configuration assignments of the populated states. This is the first observation of states with excitation energy greater than 1.5 MeV being populated following  $\alpha$  decay in nuclei outside of the  $^{208}\text{Pb}$  region.

PACS numbers: 23.60.+e, 27.70.+q, 29.30.Ep, 29.30.Kv

---

<sup>†</sup>Permanent address: Department of Physics, College of Education, University of Sulaimani, P.O. Box 334, Sulaimani, Kurdistan Region, Iraq

<sup>‡</sup>Present address: Department of Physics, University of Guelph, Guelph, Ontario N1G 2W1, Canada

<sup>§</sup>Present address: Physics Division, Argonne National Laboratory, Argonne, Illinois 60439, USA

<sup>¶</sup>Present address: ELINP, Horia Hulubei National Institute for Research in Physics and Nuclear Engineering, Bucharest-Măgurele, Romania

<sup>\*\*</sup>Present address: Institute of Physics, Slovak Academy of Sciences, SK-84511 Bratislava, Slovakia

<sup>††</sup>Present address: Department of Physics, KTH-Royal Institute of Technology, SE-10691 Stockholm, Sweden

<sup>‡‡</sup>Present address: CERN, CH-1211 Geneva 23, Switzerland

<sup>§§</sup>Present address: School of Engineering and Computing, University of the West of Scotland, Paisley, PA1 2BE, United Kingdom

<sup>¶¶</sup>Present address: Oliver Lodge Laboratory, University of Liverpool, Liverpool, L69 7ZE, United Kingdom

<sup>\*\*\*</sup>Present address: Physics Division, Argonne National Laboratory, Argonne, Illinois 60439, USA

\*Electronic address: ep@ns.ph.liv.ac.uk

## CORRESPONDING AUTHOR:

Dr Edward Parr

### Address:

Oliver Lodge Laboratory,  
University Liverpool,  
Liverpool,  
L69 7ZE,  
UK

Email: ep@ns.ph.liv.ac.uk

## I. INTRODUCTION

The establishment of  $^{146}_{64}\text{Gd}_{82}$  as a semi-doubly-magic nucleus [1–3] has meant that the neighbouring nuclei are excellent cases in which to test the nuclear shell model for systems with small numbers of valence nucleons. Notable successes of the shell model in this region have been the excellent reproduction of observed level energies, as well as  $B(E2)$  values from decaying seniority isomers in the  $N = 82$  isotones  $^{148}\text{Dy}$ ,  $^{149}\text{Ho}$ ,  $^{150}\text{Er}$ ,  $^{151}\text{Tm}$ ,  $^{152}\text{Yb}$ ,  $^{153}\text{Lu}$  and  $^{154}\text{Hf}$  above  $Z = 64$  [4–12]. Here, low-lying levels are largely determined by valence protons in the  $h_{11/2}$ ,  $s_{1/2}$  and  $d_{3/2}$  shells.

For the even  $N = 82$  isotones with  $n$  valence protons outside of the core  $^{146}\text{Gd}$ , the shell model predicts five positive-parity states with  $J^\pi = 2^+$ ,  $4^+$ ,  $6^+$ ,  $8^+$ ,  $10^+$  formed by the seniority  $s = 2$ ,  $\pi(h_{11/2})^n$  multiplet, and a full-paired,  $s = 0$  ground state. All, or some, of these multiplet states have been observed in the even isotones mentioned and agree very well with predictions of the shell model. Additionally, three negative-parity states in each even isotone have been consistently observed. These have been assigned as  $\pi(h_{11/2}d_{5/2}^{-1})3^-$  particle-hole octupole states, from the excitation of a  $d_{5/2}$  proton from below the  $Z = 64$  energy gap, and  $\pi(h_{11/2}^{-1}s_{1/2})5^-$  and  $\pi(h_{11/2}^{-1}d_{3/2})7^-$  states, from the breaking of a  $h_{11/2}$  pair. In the odd isotones the additional  $\pi(h_{11/2})$  proton would be expected to couple to these configurations, producing  $J^\pi = 15/2^-, 19/2^-, 23/2^-, 27/2^-$  seniority 3,  $\pi(h_{11/2})^n$  multiplet states and  $J^\pi = 15/2^+, 19/2^+$  and  $23/2^+$  opposite-parity states. These, again have been observed in the odd isotones listed above, with the energies of the multiplet states being well reproduced by shell-model calculations.

An experimental observable which has not previously been utilised to study these states, however, is  $\alpha$ -decay fine structure. The study of fine structure provides  $\alpha$ -decay reduced hindrance factors (proportional to the inverse of the reduced decay widths) which are a measure of the overlap of the initial and final nuclear wavefunctions in an  $\alpha$ -decay process; these then indicate the similarities of configurations of the initial and final states. The comparison of reduced hindrance factors to different levels in product nuclei from the same initial state can also, therefore, provide evidence for the similarity, or otherwise, of these final states. Additionally,  $\alpha$ -decay fine-structure studies are useful in constructing, or confirming, level schemes populated in product nuclei.

The main experimental challenge in populating states in  $N = 82$  nuclei via  $\alpha$  decay is the large excitation energies of their  $s > 1$  states, of around 1.5 MeV. The reduction in  $Q_\alpha$  leads to a dramatic drop in  $\alpha$  branching ratios to the states. A possible solution to this problem is to search for  $\alpha$ -decaying branches from high-energy isomeric states. Although the reduction in  $Q_\alpha$  is the same, the higher energies of the possible  $\alpha$  decays populating excited states allows these branches to compete with those

to the ground states. This phenomenon has previously been observed in the region above  $^{208}\text{Pb}$ . In that region there have been five examples of nuclei whereby a high-energy isomeric state has been observed to  $\alpha$  decay to a state with  $E_{excitation} \gtrsim 1.5$  MeV; specifically these from  $^{211}\text{Po}$  [13, 14],  $^{212}\text{Po}$  [14],  $^{214}\text{Ra}$  [15],  $^{216}\text{Ra}$  [16] and  $^{217}\text{Pa}$  [17].

This paper presents the results of a study of the  $\alpha$  decay fine-structure populating excited states in the  $N = 82$  nuclei  $^{151}\text{Tm}$  and  $^{152}\text{Yb}$  from the high-spin isomers in  $^{155}\text{Lu}$  ( $J^\pi = 25/2^-$ ) and  $^{156}\text{Hf}$  ( $J^\pi = 8^+$ ), respectively. This is the first time  $\alpha$ -decay fine structure to states with seniority  $s > 1$  configurations in  $N = 82$  isotones above  $^{146}\text{Gd}$  has been reported. Previously only the  $\alpha$  decay to single-proton states in odd isotones has been observed [18–22]. It is also the first report of states with  $E_{excitation} \gtrsim 1.5$  MeV being populated following  $\alpha$  decay in a different region to that just above  $^{208}\text{Pb}$ .

## II. PREVIOUS STUDIES

### A. Excited states in $^{151}_{69}\text{Tm}$ and $^{152}_{70}\text{Yb}$

Excited states in  $^{151}\text{Tm}$  were first studied using  $\gamma$ -ray spectroscopy following the decay of a  $J^\pi = 27/2^-$ ,  $T_{1/2} = 470(50)$  ns isomer [7]. Four  $\gamma$ -ray transitions were observed, and from intensity comparisons were determined to have stretched E2 multipolarity. This allowed for the  $\pi(h_{11/2})^5$ ,  $s = 3$ , multiplet sequence to be established. A subsequent investigation identified the  $\gamma$  rays emitted promptly following the production of  $^{151}\text{Tm}$  via fusion evaporation, as well as those from the decay of the isomer [10]. The initial level scheme below the isomer was confirmed, as well as the sequence of three positive-parity states described in Sec. I. Due to the low statistics some of these positive-parity states could only be placed tentatively in the work of Ref. [10].

The excited states in  $^{152}\text{Yb}$  were first investigated by studying prompt  $\gamma$  rays, as well as those emitted following the decay of a  $J^\pi = 10^+$ ,  $T_{1/2} = 39(5)$   $\mu\text{s}$  isomer [10]. A cascade of five  $\gamma$  rays was used to identify levels from the  $\pi(h_{11/2})^6$ ,  $s = 2$ , multiplet sequence, as well as the three negative-parity states. A further investigation was carried out detecting  $\gamma$  rays and conversion electrons emitted following the decay of the isomer in  $^{152}\text{Yb}$  [9]. From this work, the multiplicities of all the transitions were determined, allowing for a firm assignment of all energies, spins and parities of the levels. The lowest three transitions were also observed following the  $\beta$  decay of  $^{152}\text{Lu}$  [23].

### B. High-spin isomers in $^{155}_{71}\text{Lu}(25/2^-)$ and $^{156}_{72}\text{Hf}(8^+)$

High-spin isomers in  $^{155}\text{Lu}$  and  $^{156}\text{Hf}$  were first observed via their  $\alpha$  decays to the ground states of  $^{151}\text{Tm}$  and  $^{152}\text{Yb}$ , respectively [24]. The decay half-lives and

$\alpha$ -particle energies were measured to be 2.7(3) ms and 7408(10) keV for  $^{155}\text{Lu}$  and 0.52(16) ms and 7804(15) keV for  $^{156}\text{Hf}$ . Although identified as decaying isomeric states with excitation energies between  $\sim 2$  and 3 MeV, they were not, at the time, attributed to specific nuclei. Subsequent discussion, however, assigned them as states in  $^{155}\text{Lu}$  and  $^{156}\text{Hf}$  in Refs. [25, 26]; the latter reference also giving new values of  $E_\alpha = 7379(15)$  keV and  $T_{1/2} = 2.60(7)$  ms for the decay from the isomer in  $^{155}\text{Lu}$ . Finally, the  $\alpha$  decays from both of the isomers were studied and reported in Ref. [21]. Values of  $E_\alpha = 7390(5)$  keV,  $T_{1/2} = 2.71(3)$  ms and  $E_\alpha = 7782(4)$  keV,  $T_{1/2} = 0.52(1)$  ms were given for the  $\alpha$  decays from the  $^{155}\text{Lu}$  and  $^{156}\text{Hf}$  isomers, respectively, and the mass assignments were confirmed using  $A/q$  recoil separation. No other  $\alpha$ -decay branch or decay mode has been reported from either isomeric state.

With 8 protons and 2 neutrons above the core of  $^{146}\text{Gd}$ , the high-spin isomer in  $^{156}\text{Hf}$  has been interpreted to have a  $\nu(f_{7/2}h_{9/2})8^+$  configuration [26, 27]. The isomeric state in  $^{155}\text{Lu}$ , with an unpaired  $\pi h_{11/2}$  proton, has been interpreted to have a  $\pi(h_{11/2})^3\nu(f_{7/2}h_{9/2})25/2^-$  configuration, which includes the addition of a proton seniority 3 structure [28]. The existence of these isomers is explained by the  $8^+(25/2^-)$  state in  $^{156}\text{Hf}(^{155}\text{Lu})$  having been observed to have lower energy than that of the  $6^+(23/2^-)$  state of the  $\nu(f_{7/2})^2[\pi(h_{11/2})\nu(f_{7/2})^2]$  band [27]([28]); hence forming a spin-trap isomer. The high-spin isomeric states will subsequently be referred to as  $^{155}\text{Lu}(25/2^-)$  and  $^{156}\text{Hf}(8^+)$  in this paper.

### III. EXPERIMENTAL DETAILS

The results presented in this paper were obtained from an experiment performed at the Accelerator Laboratory of the University of Jyväskylä, Finland. The  $^{155}\text{Lu}$  and  $^{156}\text{Hf}$  nuclei were produced by a fusion-evaporation reaction using a  $^{58}\text{Ni}$  beam incident on a  $^{106}\text{Cd}$  target for around 292 hours. The  $^{58}\text{Ni}$  beam had energy of 318 MeV with an average intensity of  $\sim 6.4$  particle nA. The target was a self-supporting  $^{106}\text{Cd}$  target of thickness  $0.975 \text{ mg cm}^{-2}$ . The fusion-evaporation products were separated from other reaction products and unreacted beam ions using the RITU gas-filled recoil separator [29, 30]. They were then implanted into two double-sided silicon-strip detectors (DSSDs), which are part of the GREAT spectrometer [31], located at a focal plane of RITU. The two DSSDs each consisted of 40 horizontal and 60 vertical strips giving a total of 4800 individual pixels. An array of 28 silicon PIN diode detectors were located upstream from the DSSDs positioned to detect charged particles emitted out of the DSSDs. An array of three HPGe clover detectors surrounding the DSSDs was used to detect  $\gamma$  and X rays emitted by decaying implanted nuclei. These detectors were placed at  $\theta = 90^\circ$  to the central path of the recoils, on either side and above the DSSDs. Downstream of the DSSDs, within the vac-

uum chamber of GREAT, was a double-sided germanium strip detector. This was used to detect predominantly low-energy  $\gamma$  rays and X rays emitted following nuclear decays. At the entrance of GREAT was a multi-wire proportional counter (MWPC). This was used to measure the energy loss of incoming recoils which, along with the time-of-flight from the MWPC to the DSSDs, enabled the selection of desired recoils over incoming unreacted beam or other reaction products. For the temporal correlation of the detector signals each was timestamped in units of 10 ns [32].

### IV. DATA ANALYSIS

The data analysis was performed using the GRAIN software [33], which was developed for use with data acquired by the Total Data Readout system [32]. The DSSDs were calibrated using  $\alpha$  particles emitted by implanted evaporation residues, or those in their decay chains, produced during the experiment. The  $\alpha$  particles used were from  $^{150}\text{Dy}$  [ $E_\alpha = 4233(3)$  keV] [34],  $^{152}\text{Er}$  [ $E_\alpha = 4799(3)$  keV] [34],  $^{157}\text{Hf}$  [ $E_\alpha = 5729(4)$  keV] [21],  $^{158}\text{Ta}$  [ $E_\alpha = 6046(4)$  keV] [21] and  $^{158m}\text{W}$  [ $E_\alpha = 8286(7)$  keV] [35]. The branching ratios of the studied  $\alpha$  decays of interest in  $^{155}\text{Lu}$  and  $^{156}\text{Hf}$  were small, therefore analysis of coincidences between  $\alpha$  particles detected in the DSSDs and  $\gamma$  rays, emitted following the population of excited states in daughter nuclei, detected in the focal-plane clover-detector array was needed to identify them. The absolute efficiency for the detection of  $\gamma$  rays in the focal-plane clover-detector array was determined using GEANT4 Monte Carlo simulations.

Candidates for  $\alpha$  decays from fusion-evaporation products were identified as signals in the DSSDs which did not have coincident MWPC signals. As the recoiling nuclei were implanted close to the surface of the DSSDs a significant proportion ( $\sim 40\%$ ) of the  $\alpha$  particles were emitted out of the detectors, therefore depositing only a fraction of their energy. Some of these *escaping*  $\alpha$  particles were then detected in the PIN-diode detectors. The background signals in the DSSDs produced by the partial energy deposition of the escaping  $\alpha$  particles could, therefore, be reduced to some extent by vetoing potential  $\alpha$  particles with a coincident PIN signal. Possible  $\alpha$  decays were also correlated with a preceding recoil implantation in the same pixel of the DSSD. The incoming recoils were identified by gating on their characteristic energy loss in the MWPC and their time-of-flight from the MWPC to the DSSD. The time between the recoil and the decay was required to be up to 8.2 ms to identify  $\alpha$  decays from  $^{155}\text{Lu}(25/2^-)$  ( $T_{1/2} = 2.7$  ms) and up to 1.5 ms for those from  $^{156}\text{Hf}(8^+)$  ( $T_{1/2} = 0.52$  ms).

## V. RESULTS

The properties of  $\alpha$  decays identified in the present study are given in Table I. The table gives the following information: the  $\alpha$ -particle energies; the  $\alpha$ -decay branching ratios; the reduced decay widths; reduced hindrance factors of the decays calculated as described in Sec. VI; the spins, parities and energies of the states populated in the daughter nuclei; and the total  $Q$  values of the decays, which is the sum of the  $Q$  value of the  $\alpha$  decay and the excitation energy of the final state. Figure 1 shows the states in  $^{151}\text{Tm}$  and  $^{152}\text{Yb}$  populated following the  $\alpha$  decays of  $^{155}\text{Lu}(25/2^-)$  and  $^{156}\text{Hf}(8^+)$  reported here, as well as those from the  $^{155}\text{Lu}$  and  $^{156}\text{Hf}$  ground states.

To confirm that the  $\alpha$  decays identified are from  $^{155}\text{Lu}(25/2^-)$  and  $^{156}\text{Hf}(8^+)$ , the total  $Q$  values of the decays,  $Q_T = Q_\alpha + E_f$ , are compared with those for the  $\alpha$  decays which populate the ground states. Figure 2(a) shows  $\alpha$ -particle energies measured in the DSSDs which were identified with a recoil implantation in the same pixel up to 8.2 ms preceding them. From this spectrum  $\alpha$  particles were measured with energies  $E_\alpha = 7383(4)$  keV from  $^{155}\text{Lu}(25/2^-)$  and  $E_\alpha = 7775(5)$  keV from  $^{156}\text{Hf}(8^+)$ . These values are consistent with those previously reported in Refs. [21, 24–26] and as they were seen only in coincidence with background  $\gamma$  rays they are assumed to populate the ground states of the daughter nuclei. Also, to help identify  $\alpha$  decays from the  $^{155}\text{Lu}(25/2^-)$  and  $^{156}\text{Hf}(8^+)$  isomers the decay times for the  $\alpha\gamma$  coincidences from each of the  $\alpha$ -decaying groups are compared with those from the decays to the ground states of the daughter nuclei; shown in Fig. 3. By plotting the decay time on a logarithmic scale a distribution of universal shape with a peak value at the mean lifetime is produced, as detailed in Ref. [36]. The random correlation component, corresponding to a recoil-implantation lifetime per DSSD pixel of around 1.5 s, is also visible.

### A. $^{155}\text{Lu}(25/2^-) \rightarrow ^{151}\text{Tm}$ $\alpha$ -decay fine structure

Figure 4 shows  $\alpha\gamma$  coincidences gated for  $\alpha$  decays from  $^{155}\text{Lu}(25/2^-)$  (as detailed in Sec. IV). Spectra of  $\alpha$ -particle energies in coincidence with the three  $\gamma$  rays identified from the deexcitation of states in  $^{151}\text{Tm}$  are shown separately in Fig. 2(b-d). The  $\alpha$  particles from  $^{155}\text{Lu}(25/2^-)$  were identified with the help of the diagonal lines shown on the  $\alpha\gamma$ -coincidence spectrum in Fig. 4. The lines represent a constant  $Q_T$  value when summing the  $\gamma$ -ray energy and the  $\alpha$ -decay  $Q$  value. They represent the  $Q_T$  values between  $^{155}\text{Lu}(25/2^-)$  and the  $^{151}\text{Tm}$  ground state,  $Q[^{155}\text{Lu}(25/2^-) \rightarrow ^{151}\text{Tm}(11/2^-)]$  (dashed line), and  $J^\pi = (15/2^+)$  state 1490 keV above the ground state (as reported in Ref. [10]),  $Q[^{155}\text{Lu}(25/2^-) \rightarrow ^{151}\text{Tm}(15/2^+)]$  (dot-dashed line).

### 1. $E_\alpha = 5521$ keV

Along the  $Q[^{155}\text{Lu}(25/2^-) \rightarrow ^{151}\text{Tm}(15/2^+)]$  line in Fig. 4(a) coincidences between  $\alpha$  particles with  $E_\alpha = 5521(8)$  keV and  $\gamma$  rays with  $E_\gamma = 415$  keV are highlighted; the projection of the coincident  $\gamma$  rays is shown in Panel (b). Previously, a level has been tentatively assigned at 1905 keV with  $J^\pi = (19/2^-)$  in  $^{151}\text{Tm}$  which decays to the  $(15/2^+)$  level via the emission of a 415-keV  $\gamma$  ray [10]. It is therefore proposed that the  $\alpha$  decay associated with these coincidences directly populates this  $(19/2^+)$  level in  $^{151}\text{Tm}$  from the  $^{155}\text{Lu}(25/2^-)$  isomeric state; this also confirms the positioning of a level at 1905 keV. The DSSD spectra in coincidence with the 415- and 1490-keV  $\gamma$  rays are given in Fig. 2, Panels (b) and (c), respectively. As expected, the 5521(8)-keV  $\alpha$  particle is seen in coincidence with both of these  $\gamma$  rays. The prominent  $^{155}\text{Lu}(25/2^-)$  7383-keV contaminant peak in 2(b) is the result of random coincidences due to the high intensity of Compton-scattered 511-keV electron-positron annihilation  $\gamma$  rays over the 415-keV peak. The total decay  $Q$  value of 7572(8) keV is consistent with the  $Q$  value of 7578(4) keV for the  $\alpha$  decay to the ground state of  $^{151}\text{Tm}$ . Figure 3(a) shows the decay times of the  $\alpha\gamma$  coincidences with  $\gamma$ -ray energy 415 keV which are proposed to populate the  $(19/2^+)$  state. The distribution is in excellent agreement with that from the  $\alpha$  decays to the ground state. The large long-lived component is again caused by the background of Compton-scattered 511-keV  $\gamma$  rays.

### 2. $E_\alpha = 5928$ keV

Coincidences between  $\alpha$  particles with  $E_\alpha = 5928(5)$  keV and  $\gamma$  rays with  $E_\gamma = 1490$  keV are highlighted in Fig. 4(a), with the projected energies of the  $\gamma$  rays given in Panel (c) and  $\alpha$  particles in Fig. 2(c). These coincidences appear on the  $Q[^{155}\text{Lu}(25/2^-) \rightarrow ^{151}\text{Tm}(11/2^-)]$  line. A  $(15/2^+)$  state has previously been observed in  $^{151}\text{Tm}$  at 1490 keV which decays via  $\gamma$ -ray emission directly to the ground state [10]. It is therefore proposed that these coincidences are associated with the population, and subsequent decay, of this  $(15/2^+)$  state via the  $\alpha$  decay of  $^{155}\text{Lu}(25/2^-)$ . The total  $Q$  value of the decay is 7575(5) keV, which is consistent with the  $Q = 7578(4)$  keV value for the  $\alpha$  decay to the ground state. The distribution of decay times of these coincidences, shown in Fig. 3(b), are also consistent with the distribution of the  $\alpha$  decays to the ground state.

### 3. $E_\alpha = 5937$ keV

A small number of coincidences between  $\alpha$  particles with  $E_\alpha = 5937(15)$  keV and  $\gamma$  rays with  $E_\gamma = 1478$  keV are highlighted in Fig. 4(a), with the projection of  $\gamma$

rays given in Panel (c). These coincidences appear on the  $Q[{}^{155}\text{Lu}(25/2^-) \rightarrow {}^{151}\text{Tm}(11/2^-)]$  line. A  $15/2^-$  state has previously been observed in  ${}^{151}\text{Tm}$  at 1478 keV which decays via  $\gamma$ -ray emission directly to the ground state [7, 10]. Although there are only a small number of coincidences, the clean  $\alpha$  particle energy in coincidence with the 1478-keV  $\gamma$  rays, shown in Fig. 2(d), gives a total decay  $Q$  value of 7573(15) keV. As this is consistent with the  $Q$  value of the  $\alpha$  decay to the ground state of 7578(4) keV it is proposed that the coincidences are associated with the population of the  $15/2^-$  state at 1478 keV in  ${}^{151}\text{Tm}$ . Further evidence is also provided for this assignment by agreement of the the decay times of the four  $\alpha\gamma$  coincidence events with the distribution from the  $\alpha$  decays to the ground state, shown in Fig. 3(c).

### B. ${}^{156}\text{Hf}(8^+) \rightarrow {}^{152}\text{Yb}$ $\alpha$ -decay fine structure

Figure 5 shows  $\alpha\gamma$  coincidences gated for  $\alpha$  decays from  ${}^{156}\text{Hf}(8^+)$  (as detailed in Sec. IV). Strong contaminant coincidences from the  $\alpha$ -decay fine structure of  ${}^{155}\text{Lu}(25/2^-)$ , discussed previously, are highlighted in a dashed circle and labelled in brackets. The  $\alpha$  particles from the  ${}^{156}\text{Hf}(8^+)$  isomers were identified with the help of the diagonal line shown on the  $\alpha\gamma$ -coincidence spectrum. The line represents a constant  $Q_T$  value for the sum of the  $\alpha$ -decay  $Q$  value, calculated from the  $\alpha$ -particle energy, and the  $\gamma$ -ray energy. It is equal to the  $Q$  value between the  ${}^{156}\text{Hf}(8^+)$  isomeric state and the  ${}^{152}\text{Yb}$  ground state,  $Q[{}^{156}\text{Hf}(8^+) \rightarrow {}^{152}\text{Yb}(0^+)]$ .

#### 1. $E_\alpha = 6274$ keV

Coincidences between  $\alpha$  particles with  $E_\alpha = 6274(15)$  keV and  $\gamma$  rays with  $E_\gamma = 1531$  keV are highlighted in Fig. 5(a). Panel (b) shows the projection of  $\gamma$  rays in coincidence with 6274-keV  $\alpha$  particles (as well as those of 5942 keV to be discussed in the next section). These appear on the  $Q[{}^{156}\text{Hf}(8^+) \rightarrow {}^{152}\text{Yb}(0^+)]$  line and the  $2_1^+$  state in  ${}^{152}\text{Yb}$  has previously been identified 1531 keV above the  $0^+$  ground state [9, 10, 23]. The coincidences are therefore proposed to derive from the  $\alpha$  decay of  ${}^{156}\text{Hf}(8^+)$  to the  $2_1^+$  state in  ${}^{152}\text{Yb}$ . The  $Q_T$  value of 7971(15) keV is consistent with the value of 7980(5) keV for the  $\alpha$  decay to the ground state. Also, the decay times, shown in Fig. 3(d), compare well with the distribution for the decays to the ground state of  ${}^{152}\text{Yb}$ .

#### 2. $E_\alpha = 5942$ keV

The DSSD energies in coincidence with the 1531-keV  $\gamma$  rays are shown in Fig. 5(c). Along with the counts associated with the population of the  $2_1^+$  state there is a cluster

of three counts with an energy of 5942(15) keV. Comparison of the decay times of these three coincidences with the distribution for the decay of  ${}^{156}\text{Hf}(8^+)$  to the ground state of  ${}^{152}\text{Yb}$ , in Fig. 3(e), shows them to be consistent; implying they could be produced by the decay of  ${}^{156}\text{Hf}(8^+)$ . If these counts are assumed to be associated with the  $\alpha$  decay that populates the  $3^-$  state in  ${}^{152}\text{Yb}$  at 1890 keV [9, 10, 23], which decay via a cascade of 359- and 1531-keV transitions, then the total  $Q$  value would be 7989(15) keV for the decay. This is consistent with the value of 7980(5) keV for the  $\alpha$  decay to the ground state. It is therefore proposed that the coincidences are associated with the  $\alpha$  decay of  ${}^{156}\text{Hf}(8^+)$  to the  $3^-$  state in  ${}^{152}\text{Yb}$ . No coincidences were observed between  $\alpha$  particles with 5942 keV and 359-keV,  $3^- \rightarrow 2^+$ ,  $\gamma$  rays. Considering the low statistics of the  $\alpha\gamma$  coincidences between 5942(15)-keV  $\alpha$  particles and 1531-keV  $\gamma$  rays, only a small number if any, of these counts would be expected. As the  $\gamma$ -ray energy lies in the Compton continuum produced by the 511-keV background  $\gamma$  ray, small numbers of these  $\alpha\gamma$  would be difficult to identify; this can be seen in Fig. 4(a) and (b).

## VI. DISCUSSION: $\alpha$ -DECAY REDUCED HINDRANCE FACTORS

Table I and Fig. 1 give the reduced hindrance factors,  $HF$ , for each of the  $\alpha$  decays observed. These are found from the reduced decay widths,  $\delta^2$ , calculated using the method prescribed by Rasmussen [37], with the lowest permissible spin change for each  $\alpha$  decay considered. The reduced hindrance factors have been taken as the inverse of these reduced decay widths, scaled so that  $HF({}^{212}\text{Po} \rightarrow {}^{208}\text{Pb}) = 1$  [where  $\delta^2({}^{212}\text{Po} \rightarrow {}^{208}\text{Pb}) = 71.4$  keV]. Figure 6 shows the reduced hindrance factors of all of the  $\alpha$  decays observed from  ${}^{155}\text{Lu}(25/2^-)$  and  ${}^{156}\text{Hf}(8^+)$ , as well as those from their ground states. Populated states with analogous configurations in  ${}^{151}\text{Tm}$  and  ${}^{152}\text{Yb}$  have the same symbols.

It can be seen that the hindrance factors to states in  ${}^{151}\text{Tm}$  and  ${}^{152}\text{Yb}$  which have been previously assigned with analogous configurations are comparable. This appears to corroborate the assignments. Comparing the hindrance factors to the daughter ground states (circles) from both the ground and isomeric states of the decaying nuclei, there is roughly an order of magnitude increase for the decays from the isomers. The hindrance of an  $\alpha$  decay is determined by both the difference in nuclear structure of the initial and final states and also the pairing of the decaying state; this having a large influence on the  $\alpha$ -particle preformation factor [38]. In this case, the increase in  $HF$ s may be attributed to the weakening of pairing correlations produced by the  $\nu(f_{7/2}h_{9/2})$  configuration of the isomeric states compared with the fully paired  $\nu(f_{7/2})^2$  ground states.

For  $\alpha$  decays from the isomeric states there is again roughly an order of magnitude increase for the hindrance

factors to the first  $\pi(h_{11/2})^{5(6)}$ ,  $s = 3(2)$  multiplet excitations with  $15/2^-(2^+)$  in  $^{151}\text{Tm}(^{152}\text{Yb})$  (triangles) compared with those to the  $s = 1(0)$  ground states. This increase may be explained by nuclear-structure considerations due to the rearrangement of the  $h_{11/2}$  protons required to form the first multiplet excitation. More surprising perhaps, when considering the  $\alpha$  decays from  $^{155}\text{Lu}(25/2^-)$ , is that the hindrances to the  $15/2^+$  and  $19/2^+$  states are very similar. As they have been assigned with different structures, a  $\pi(h_{11/2}d_{5/2}^{-1})$  octupole excitation ( $15/2^+$ ) (square) and a  $\pi(h_{11/2}s_{1/2})$  proton excitation ( $19/2^+$ ) (cross), different hindrances may be expected to be observed to each of them. However, it may be the case that the populated states are both similarly *different* so as to produce comparably hindered  $\alpha$  decays. The hindrance of the decay from  $^{156}\text{Hf}(8^+)$  to the  $\pi(h_{11/2}d_{5/2}^{-1})$  (square) state in  $^{152}\text{Yb}$  is somewhat uncertain due to low statistics. However, it is consistent with that of the analogous octupole state in  $^{151}\text{Tm}$ .

Recent theoretical attempts have been made to quantify the reduction of pairing in multi-quasiparticle isomers which causes an increase in  $\alpha$ -decay hindrance from these states compared with those from ground states [38, 39]. However, the effects of nuclear structure and pairing changes are difficult to deconvolute. Experimental data for the fine structure in  $\alpha$  decay from isomeric states in this region, combined with those from nuclei around  $^{208}\text{Pb}$ , could prove helpful in determining the effects of reduced pairing on  $\alpha$ -decay hindrances.

## VII. SUMMARY AND FUTURE WORK

The  $\alpha$ -decay fine structure of high-spin isomers in  $^{155}\text{Lu}(25/2^-)$  and  $^{156}\text{Hf}(8^+)$  has been studied using  $\alpha\gamma$ -coincidence analysis. Three new  $\alpha$  decays from  $^{155}\text{Lu}(25/2^-)$  and two from  $^{156}\text{Hf}(8^+)$  have been identified which populate states in the  $N = 82$  isotones  $^{151}\text{Tm}$  and  $^{152}\text{Yb}$ . This has allowed confirmation of the previously tentative level at 1905 keV assigned with  $J^\pi = (19/2^+)$ . The populated states had previously been interpreted as various proton seniority  $s > 1$  structures which are well described by the shell model. An analysis of the hindrance factors of the  $\alpha$ -decays populating these states was consistent with the structural assignments previously made.

This is the first report of states with such high energies ( $E_{excitation} \gtrsim 1.5$  MeV) being populated following  $\alpha$  decay outside the region above  $^{208}\text{Pb}$ . As well as providing a challenge for theorists to describe these  $\alpha$ -decay branches in both regions there is also scope for further experimental investigation in nuclei above  $^{146}\text{Gd}$ . For example another  $\alpha$ -decaying high-energy spin-trap isomer in the  $N = 84$  isotone chain is known to exist in  $^{158}\text{W}$  [26], and significant branches populating states in  $^{154}\text{Hf}$  could be observed. Additionally, a hint of a high-energy  $\alpha$ -decaying isomeric state was reported in  $^{157}\text{Ta}$  [21], but

the apparent similarity of its  $\alpha$ -decay energy and half-life to that of the  $\alpha$  decay from  $^{156}\text{Hf}(8^+)$  have meant this has not been possible to confirm. The observation of  $\alpha$ -decay branches from this isomer to known excited states in  $^{153}\text{Lu}$  would provide confirmation of its existence.

This work has been supported by the United Kingdom Science and Technology Facilities Council (S.T.F.C.); the Academy of Finland under the Finnish Center of Excellence Programme (2012- 2017); the EU 7<sup>th</sup> framework programme, Project No. 262010 (ENSAR); the Slovak Research and Development Agency under contract No. APVV-15-0225; and the Slovak grant agency VEGA (contract nr. 2/0129/17). The authors also thank the GAMMAPOOL European Spectroscopy Resource for the loan of the detectors of the JUROGAM II array.

TABLE I:  $\alpha$ -particle energies,  $E_\alpha$ , branching ratios,  $b_\alpha$ , reduced decay widths,  $\delta^2$ , and reduced hindrance factors,  $HF$ , of  $\alpha$  decays from  $^{155}\text{Lu}(25/2^-)$  and  $^{156}\text{Hf}(8^+)$  to final states with  $J_f^\pi$  at energies  $E_f$  in  $^{151}\text{Tm}$  and  $^{152}\text{Yb}$ . Total decay  $Q$  values,  $Q_T$ , are given by  $Q_\alpha + E_f$ .

$E_\alpha$ (keV)	$J_f^\pi$	$E_f$ (keV)	$Q_T$ (keV)	$b_\alpha$ (%)	$\delta^2$ (keV)	$HF$
$^{155}\text{Lu}(25/2^-)$						
7383(4)	11/2 <sup>-</sup>	0	7578(4)	99.964(6)	3.63(10)	19.4(5)
5937(15)	15/2 <sup>-</sup>	1478	7573(15)	2.4(13) $\times 10^{-3}$	0.22(12)	320(170)
5928(5)	(15/2 <sup>+</sup> )	1490	7575(5)	2.8(6) $\times 10^{-2}$	0.87(19)	80(17)
5521(8)	(19/2 <sup>+</sup> )	1905	7572(8)	5.8(16) $\times 10^{-3}$	1.2(3)	57(16)
$^{156}\text{Hf}(8^+)$						
7775(5)	0 <sup>+</sup>	0	7980(5)	99.990(4)	3.87(14)	18.2(6)
6274(15)	2 <sup>+</sup>	1531	7971(15)	6.4(30) $\times 10^{-3}$	0.46(22)	150(70)
5942(15)	3 <sup>-</sup>	1890	7989(15)*	3.8(23) $\times 10^{-3}$	1.7(10)	45(25)

\* Calculated assuming  $\alpha$  decay populates known 3<sup>-</sup> state at 1890.1(6) keV reported in Ref. [23].

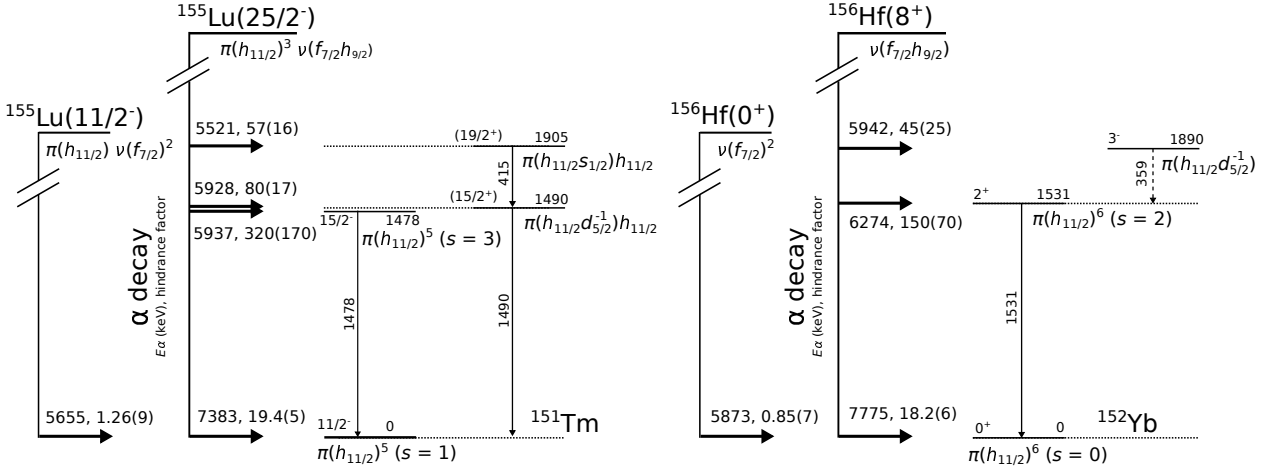


FIG. 1: Level schemes of  $^{151}\text{Tm}$  and  $^{152}\text{Yb}$  populated following the  $\alpha$  decays of the  $^{155}\text{Lu}$   $J^\pi = 25/2^-$  isomer and ground state and the  $^{156}\text{Hf}$   $J^\pi = 8^+$  isomer and ground state, respectively. The spins, parities and energies of each level are given along with the energies of the transitions. For each  $\alpha$  decay the  $\alpha$ -particle energy and reduced hindrance factors are given from the results of the present work and the state populated is also indicated. The configurations which have previously been assigned to each state (see text for details) are shown.

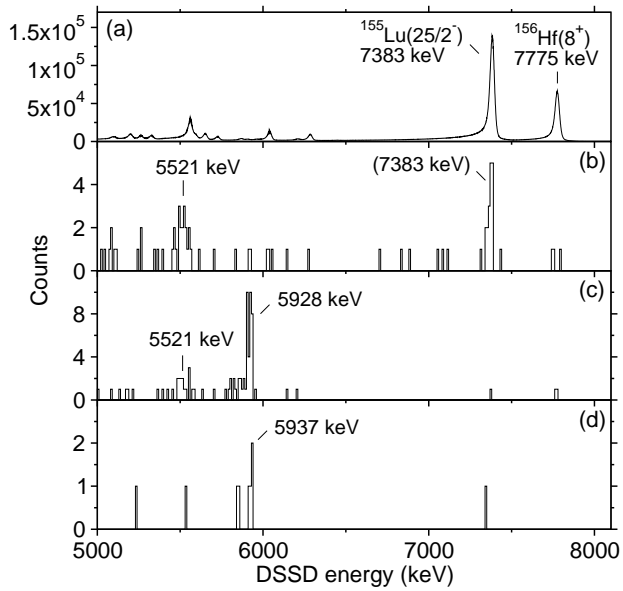


FIG. 2: DSSD  $\alpha$ -particle energy spectra recorded up to 8.2 ms after the identification of a recoil implantation in the same DSSD pixel. Panel (a) shows all  $\alpha$ -particle energies. The other panels show  $\alpha$ -particle energies in coincidence with 415- (b), 1490- (c) and 1478-keV (d)  $\gamma$  rays identified from  $^{151}\text{Tm}$ .

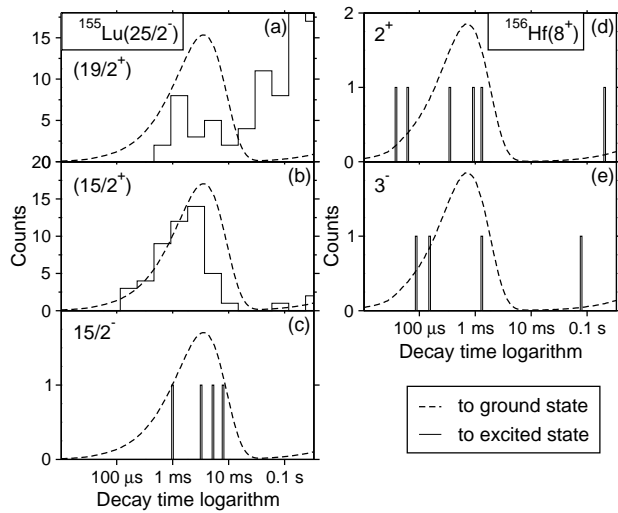


FIG. 3: Decay times for the  $\alpha$  decay identified from  $^{155}\text{Lu}(25/2^-)$  to the  $(19/2^+)$  (a),  $(15/2^+)$  (b) and  $15/2^-$  (c) states in  $^{151}\text{Tm}$  and from  $^{156}\text{Hf}(8^+)$  to the  $2^+$  (d) and  $3^-$  (e) states in  $^{152}\text{Yb}$ . Also shown as a dashed line on each panel is the distribution of the decay times from the respective isomer to the ground state. These have been scaled for comparison with the weaker branches.

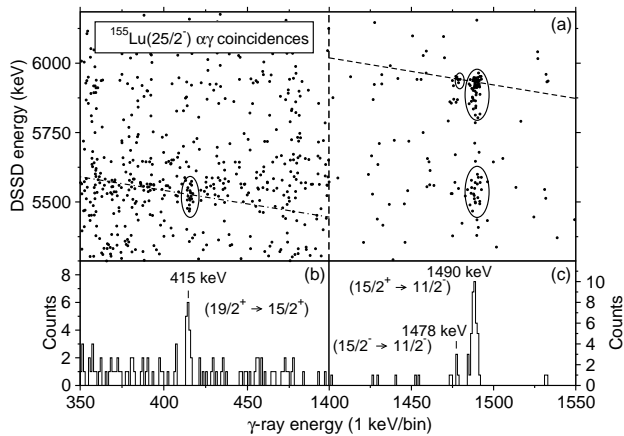


FIG. 4: Energies of coincident  $\alpha$  particles and  $\gamma$  rays measured following the decay of  $^{155}\text{Lu}(25/2^-)$ . The diagonal lines on Panel (a) represent a constant energy for the sum of the  $\alpha$ -decay  $Q$  value, calculated from the  $\alpha$ -particle energy, and the  $\gamma$ -ray energy; the energies represented are those between the  $^{155}\text{Lu}(25/2^-)$  isomeric state and both the ground state (dashed line) and excited state at 1490 keV (dot-dashed line) in  $^{151}\text{Tm}$ . The  $\alpha\gamma$  coincidences identified are circled and the  $\gamma$ -ray projections in coincidence with the 5521(8)-keV (b) and the 5928(5)- or 5937(15)-keV (c)  $\alpha$  particles are shown.

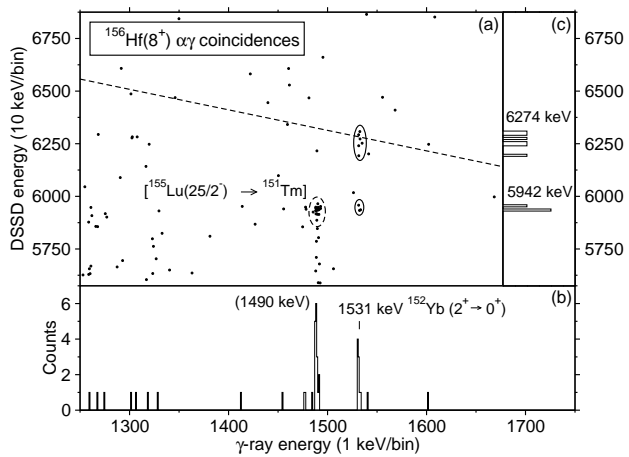


FIG. 5: Energies of coincident  $\alpha$  particles and  $\gamma$  rays measured following the decay of  $^{156}\text{Hf}(8^+)$ . The diagonal line on Panel (a) represents a constant energy for the sum of the  $\alpha$ -decay  $Q$  value, calculated from the  $\alpha$ -particle energy, and the  $\gamma$ -ray energy; the energy represents that between the  $^{156}\text{Hf}(8^+)$  isomeric state and the ground state of  $^{152}\text{Yb}$ . The  $\alpha\gamma$  coincidences identified from  $^{156}\text{Hf}(8^+)$  are circled with contaminant coincidences from  $^{155}\text{Lu}(25/2^-)$  also labelled. Also shown are the  $\gamma$ -ray energies in coincidence with the 5942(15)- or 6274(15)-keV  $\alpha$  particles (b) and the  $\alpha$ -particle energies in coincidence with the 1531-keV  $\gamma$  rays (c).

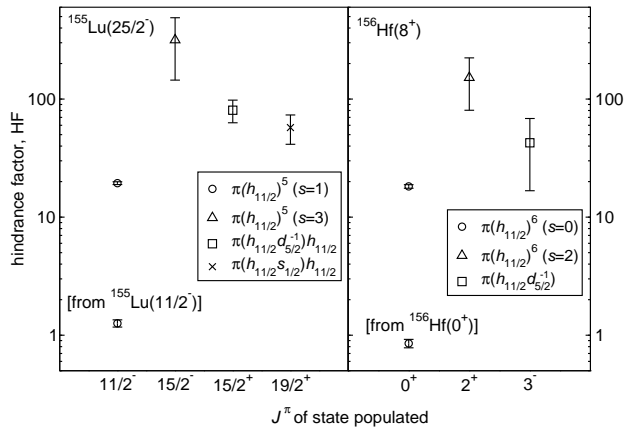


FIG. 6: Reduced hindrance factors of the  $\alpha$  decays from the  $^{155}\text{Lu}(25/2^-)$  and  $^{156}\text{Hf}(8^+)$  isomers (except where labelled) to states in  $^{151}\text{Tm}$  and  $^{152}\text{Yb}$ , respectively, with  $J^\pi$  shown on the x axis. The configurations assigned to each of the states populated is indicated and analogous states in  $^{151}\text{Tm}$  and  $^{152}\text{Yb}$  have the same symbols.

- [1] M. Ogawa, R. Broda, K. Zell, P. J. Daly, and P. Kleinheinz. *Phys. Rev. Lett.*, **41**:289–292, (1978).
- [2] P. Kleinheinz, S. Lunardi, M. Ogawa, and M. R. Maier. *Z. Phys. A: At. Nucl.*, **284**(1):351–352, (1978).
- [3] P. Kleinheinz, M. Ogawa, R. Broda, P. J. Daly, D. Haenni, H. Beuscher, and A. Kleinrahm. *Z. Phys. A: At. Nucl.*, **286**(1):27–29, (1978).
- [4] P. J. Daly, P. Kleinheinz, R. Broda, A. M. Stefanini, S. Lunardi, H. Backe, L. Richter, R. Willwater, and F. Weik. *Z. Phys. A: At. Nucl.*, **288**(1):103–104, (1978).
- [5] J. Wilson, S. R. Faber, P. J. Daly, I. Ahmad, J. Borggreen, P. Chowdhury, T. L. Khoo, R. D. Lawson, R. K. Smither, and J. Blomqvist. *Z. Phys. A: At. Nucl.*, **296**(2):185–186, (1980).
- [6] E. Nolte, G. Colombo, S. Z. Gui, G. Korschinek, W. Schollmeier, P. Kubik, S. Gustavsson, R. Geier, and H. Morinaga. *Z. Phys. A: At. Nucl.*, **306**:211–222, (1982).
- [7] H. Helppi, Y. H. Chung, P. J. Daly, S. R. Faber, A. Pakkanen, I. Ahmad, P. Chowdhury, Z. W. Grabowski, T. L. Khoo, R. D. Lawson, and J. Blomqvist. *Phys. Lett. B*, **115**(1):11–14, (1982).
- [8] Y. H. Chung, P. J. Daly, H. Helppi, R. Broda, Z. W. Grabowski, M. Kortelahti, J. McNeill, A. Pakkanen, P. Chowdhury, R. V. F. Janssens, T. L. Khoo, and J. Blomqvist. *Phys. Rev. C*, **29**:2153–2159, (1984).
- [9] D. Nisius, R. V. F. Janssens, I. G. Bearden, R. H. Mayer, I. Ahmad, P. Bhattacharyya, B. Crowell, M. P. Carpenter, P. J. Daly, C. N. Davids, Z. W. Grabowski, D. J. Henderson, R. G. Henry, R. Hermann, T. L. Khoo, T. Lauritsen, H. T. Penttilä, L. Ciszewski, and C. T. Zhang. *Phys. Rev. C*, **52**:1355–1360, (1995).
- [10] E. Nolte, G. Korschinek, and Ch. Setzensack. *Z. Phys. A: At. Nucl.*, **309**(1):33–40, (1982).
- [11] J. H. McNeill, J. Blomqvist, A. A. Chishti, P. J. Daly, W. Gelletly, M. A. C. Hotchkis, M. Piiparinen, B. J. Varley, and P. J. Woods. *Phys. Rev. Lett.*, **63**:860–863, (1989).
- [12] J. H. McNeill, A. A. Chishti, P. J. Daly, W. Gelletly, M. A. C. Hotchkis, M. Piiparinen, B. J. Varley, P. J. Woods, and J. Blomqvist. *Z. Phys. A: At. Nucl.*, **344**(4):369–379, (1993).
- [13] W. Jentschke, A. C. Juveland, and G. H. Kinsey. *Phys. Rev.*, **96**:231–232, (1954).
- [14] I. Perlman, F. Asaro, A. Ghiorso, A. Larsh, and R. Lattimer. *Phys. Rev.*, **127**:917–922, (1962).
- [15] P. Kuusiniemi, F. P. Heßberger, D. Ackermann, S. Antalic, S. Hofmann, K. Nishio, B. Sulignano, I. Kojouharov, and R. Mann. *Eur. Phys. J. A*, **30**(3):551–559, (2006).
- [16] T. Nomura, K. Hiruta, M. Yoshie, H. Ikezoe, T. Fukuda, and O. Hashimoto. *Phys. Lett. B*, **58**(3):273–276, (1975).
- [17] F. P. Heßberger, S. Hofmann, I. Kojouharov, D. Ackermann, S. Antalic, P. Cagarda, B. Kindler, B. Lommel, R. Mann, A. G. Popeko, S. Saro, J. Uusitalo, and A. V. Yeremin. *Eur. Phys. J. A*, **15**(3):335–342, (2002).
- [18] C. F. Liang, P. Paris, P. Kleinheinz, B. Rubio, M. Piiparinen, D. Schardt, A. Plochocki, and R. Barden. *Phys. Lett. B*, **191**(3):245–248, (1987).
- [19] K. S. Toth, P. A. Wilmarth, J. M. Nitschke, R. B. Firestone, K. Vierinen, M. O. Kortelahti, and F. T. Avignone. *Phys. Rev. C*, **38**:1932–1935, (1988).
- [20] K. S. Toth, K. S. Vierinen, M. O. Kortelahti, D. C. Sousa, J. M. Nitschke, and P. A. Wilmarth. *Phys. Rev. C*, **44**:1868–1877, (1991).
- [21] R. D. Page, P. J. Woods, R. A. Cunningham, T. Davinson, N. J. Davis, A. N. James, K. Livingston, P. J. Sellin, and A. C. Shotter. *Phys. Rev. C*, **53**:660–670, (1996).
- [22] R. J. Irvine, C. N. Davids, P. J. Woods, D. J. Blumenthal, L. T. Brown, L. F. Conticchio, T. Davinson, D. J. Henderson, J. A. Mackenzie, H. T. Penttilä, D. Seweryniak, and W. B. Walters. *Phys. Rev. C*, **55**:R1621–R1624, (1997).
- [23] K. S. Toth, D. C. Sousa, J. M. Nitschke, and P. A. Wilmarth. *Phys. Rev. C*, **35**:310–314, (1987).
- [24] S. Hofmann, W. Faust, G. Münzenberg, W. Reisdorf, P. Armbruster, K. Güttner, and H. Ewald. *Z. Phys. A: At. Nucl.*, **291**(1):53–70, (1979).
- [25] S. Hofmann, W. Reisdorf, G. Münzenberg, F. P. Heßberger, J. R. H. Schneider, and P. Armbruster. *Z. Phys. A: At. Nucl.*, **305**(2):111–123, (1982).
- [26] S. Hofmann, P. Armbruster, G. Berthes, T. Faestermann, A. Gillitzer, F. P. Heßberger, W. Kurcewicz, G. Münzenberg, K. Poppensieker, H. J. Schött, and I. Zychor. *Z. Phys. A: At. Nucl.*, **333**(1):107–108, (1989).
- [27] D. Seweryniak, J. Uusitalo, P. Bhattacharyya, M. P. Carpenter, J. A. Cizewski, K. Y. Ding, C. N. Davids, N. Fotiades, R. V. F. Janssens, T. Lauritsen, C. J. Lister, A. O. Macchiavelli, D. Nisius, P. Reiter, W. B. Walters, and P. J. Woods. *Phys. Rev. C*, **71**:054319, (2005).
- [28] R. J. Carroll, B. Hadinia, C. Qi, D. T. Joss, R. D. Page, J. Uusitalo, K. Andgren, B. Cederwall, I. G. Darby, S. Eckhauudt, T. Grahn, C. Gray-Jones, P. T. Greenlees, P. M. Jones, R. Julin, S. Juutinen, M. Leino, A.-P. Leppänen, M. Nyman, J. Pakarinen, P. Rakhila, M. Sandzelius, J. Sarén, C. Scholey, D. Seweryniak, and J. Simpson. *Phys. Rev. C*, **94**:064311, (2016).
- [29] M. Leino. *Nucl. Instrum. Methods Phys. Res., Sect. B*, **126**(1-4):320, (1997).
- [30] J. Uusitalo, P. Jones, P. Greenlees, P. Rakhila, M. Leino, A. N. Andreyev, P. A. Butler, T. Enqvist, K. Eskola, T. Grahn, R.-D. Herzberg, F. P. Heßberger, R. Julin, S. Juutinen, A. Keenan, H. Kettunen, P. Kuusiniemi, A.-P. Leppnen, P. Nieminen, R. Page, J. Pakarinen, and C. Scholey. *Nucl. Instrum. Methods Phys. Res., Sect. B*, **204**:638, (2003).
- [31] R. D. Page, A. N. Andreyev, D. E. Appelbe, P. A. Butler, S. J. Freeman, P. T. Greenlees, R.-D. Herzberg, D. G. Jenkins, G. D. Jones, P. Jones, D. T. Joss, R. Julin, H. Kettunen, M. Leino, P. Rakhila, P. H. Regan, J. Simpson, J. Uusitalo, S. M. Vincent, and R. Wadsworth. *Nucl. Instrum. Methods Phys. Res., Sect. B*, **204**:634, (2003).
- [32] I. H. Lazarus, E. E. Appelbe, P. A. Butler, P. J. Coleman-Smith, J. R. Cresswell, S. J. Freeman, R. D. Herzberg, I. Hibbert, D. T. Joss, S. C. Letts, R. D. Page, V. F. E. Pucknell, P. H. Regan, J. Sampson, J. Simpson, J. Thornhill, and R. Wadsworth. *IEEE Trans. Nucl. Sci.*, **48**:567, (2001).
- [33] P. Rakhila. *Nucl. Instrum. Methods Phys. Res., Sect. A*, **595**(3):637, (2008).
- [34] J. D. Bowman, R. E. Eppley, and E. K. Hyde. *Phys. Rev. C*, **25**:941–951, (1982).

- [35] H. Mahmud, C. N. Davids, P. J. Woods, T. Davinson, D. J. Henderson, R. J. Irvine, D. Seweryniak, and W. B. Walters. *Phys. Rev. C*, **62**:057303, (2000).
- [36] K. H. Schmidt, C. C. Sahm, K. Pielenz, and H. G. Clerc. *Z. Phys. A: At. Nucl.*, **316**(1):19–26, (1984).
- [37] J. O. Rasmussen. *Phys. Rev.*, **113**:1593–1598, (1959).
- [38] J. Rissanen, R. M. Clark, A. O. Macchiavelli, P. Fallon, C. M. Campbell, and A. Wiens. *Phys. Rev. C*, **90**:044324, (2014).
- [39] R. M. Clark and D. Rudolph. *Phys. Rev. C*, **97**:024333, (2018).